

High-Order Accurate Monotone Compact Running Scheme for Multidimensional Hyperbolic Equations

B. V. Rogov^{a, b}

^a Keldysh Institute of Applied Mathematics, Russian Academy of Sciences, Miusskaya pl. 4, Moscow, 125047 Russia

^b Moscow Institute of Physics and Technology, Institutskii per. 9, Dolgoprudnyi, Moscow oblast, 141700 Russia

e-mail: rogov@post.ru

Received May 21, 2012

Abstract—A high-order accurate monotone compact difference scheme proposed earlier by the author for one-dimensional nonstationary hyperbolic equations is extended to multidimensional equations. The resulting scheme is fourth-order accurate in space on a compact stencil and third-order accurate in time. Additionally, the scheme is conservative, absolutely stable, and efficient and can be solved using the running calculation method in space. By computing initial–boundary value problems for the linear advection equation and the nonlinear Hopf equation on refined meshes, it is shown that the orders of grid convergence of the multidimensional scheme are close to the corresponding orders of accuracy in independent variables. For the propagation of a two-dimensional rectangular pulse and the Hopf equation with a discontinuous solution, the multidimensional scheme is shown to inherit the monotonicity of its one-dimensional counterpart.

DOI: 10.1134/S0965542513020097

Keywords: multidimensional hyperbolic equations, compact difference schemes, monotonicity, conservation, running calculation scheme.

1. INTRODUCTION

Hyperbolic equations and systems of equations comprise a considerable part of mathematical models used in various applications [1]. Among them, a wide class of problems is related to finding weak solutions, which are described by piecewise smooth functions and can have jumps. High-order accurate shock-capturing schemes that are monotone [1] and conservative [2] are widely used for the numerical solution of such problems. In a relatively recent survey [3] concerning the construction of high-order accurate monotone conservative difference schemes for hyperbolic equations, it was noted that a promising direction in the development of such schemes is to use schemes with a compact spatial stencil, i.e., compact schemes [4]. In the class of compact schemes, symmetric ones of even order of accuracy in space are of greatest interest, because they have an important property, namely, for a hyperbolic system of conservation laws, the order of classical approximation for smooth solutions is equal to the order of weak approximation for discontinuous solutions [5].

In [6–8] for quasilinear one-dimensional equations and systems of equations of the hyperbolic type, bicomact difference schemes on a two-point stencil were proposed that are fourth-order accurate in space. These schemes are absolutely stable, conservative, and monotone for local Courant numbers $\kappa \geq 1/4$ [7, 8]. They make no use of artificial viscosity (see, e.g., [9]) or monotone procedures in the form of flux limiters (see, e.g., [10]). Moreover, they are efficient and can be solved using the running calculation method.

In this paper, bicomact difference schemes [6–8] are generalized to multidimensional hyperbolic equations. Like their one-dimensional counterparts, the generalized schemes have important properties, such as the high order of accuracy in space and time, absolute stability, conservation, and efficiency. These schemes can be solved using the running calculation method; i.e., they are easy to implement. Following the technique of [11] as applied to initial–boundary value problems for the linear advection equation and the nonlinear Hopf equation on refined meshes, we show that the orders of grid convergence of the multidimensional schemes are close to the corresponding orders of their approximation in independent variables. For the propagation of a two-dimensional rectangular pulse and an initial–boundary value problem for the Hopf equation with a discontinuous solution, it is also shown that the multidimensional schemes inherit the monotonicity of their one-dimensional analogues.

2. COMPACT SCHEME FOR A ONE-DIMENSIONAL NONSTATIONARY HYPERBOLIC EQUATION

First, we consider an initial–boundary value problem for a one-dimensional scalar quasilinear hyperbolic equation written in conservative form:

$$\begin{aligned} L_1 u &= 0, \quad L_1 u \equiv \frac{\partial u}{\partial t} + \frac{\partial F(u)}{\partial x}, \quad a(u) = \frac{dF(u)}{du} > 0, \\ u(x, 0) &= u^0(x), \quad x \geq 0; \quad u(0, t) = \mu(t), \quad t > 0. \end{aligned} \quad (1)$$

Let us briefly describe the basic ideas underlying the construction of running compact schemes [6–8] as applied to problem (1), which are used below to develop similar schemes for a multidimensional version of this problem.

The schemes proposed in [6–8] have a compact stencil and are fourth-order accurate in x . They are constructed using the method of lines and an integro-interpolation method. For this purpose, on the interval $[0, \infty)$, we introduce a basic nonuniform grid $\omega_x = \{x_j, j \geq 0\}$ consisting of integer nodes and an additional grid $\omega'_x = \{x_{j+1/2}, j \geq 0\}$ consisting of half-integer nodes. The values of the sought grid function at the half-integer nodes $u_{j+1/2}$ are treated as auxiliary in the construction of a high-order accurate running difference scheme for determining u_j at integer nodes. Discretizing the spatial derivative on the stencil consisting of two integer nodes x_j and x_{j+1} and the half-integer node $x_{j+1/2}$ yields two differential-difference equations that hold up to $O(h_{x,j+1}^4)$ for the exact solution of Eq. (1), where $h_{x,j+1} = x_{j+1} - x_j$ is the spatial step of the scheme. The first of these equations has the form

$$\frac{1}{6} \frac{d}{dt} (u_{j+1} + 4u_{j+1/2} + u_j) + \frac{1}{h_{x,j+1}} (F_{j+1} - F_j) = 0, \quad F_j = F(u_j), \quad j \geq 0 \quad (2)$$

and approximates the baseline equation (1) on the grid. The second equation is

$$\frac{d}{dt} (u_{j+1} - u_j) + \frac{4}{h_{x,j+1}} (F_{j+1} - 2F_{j+1/2} + F_j) = 0, \quad F_{j+1/2} = F(u_{j+1/2}), \quad j \geq 0 \quad (3)$$

and approximates the following differential consequence of Eq. (1):

$$\frac{\partial}{\partial x} (L_1 u) = 0. \quad (4)$$

Apparently, the idea of using equations of type (4) as differential consequences for the design of high-order accurate conservative compact schemes was first proposed in [12]. However, in contrast to [12], the values of u at half-integer nodes rather than its spatial derivatives at integer nodes were used in [6–8] as additional sought grid functions in the construction of a compact scheme.

If the function $u_j(t)$ is given (at $j = 0$, it is known from the boundary condition), then Eqs. (2) and (3) are used to determine the unknown functions $u_{j+1/2}(t)$ and $u_{j+1}(t)$. This means that $u_{j+1}(t)$ is determined from $u_j(t)$ with the help of the running calculation algorithm, while $u_{j+1/2}(t)$ is an auxiliary function in this algorithm.

Equations (2) and (3) can be written in operator form if we introduce the symmetric difference operators (see [4])

$$\begin{aligned} \Delta_0^x u_{j+1/2} &= u_{j+1} - u_j, \quad \Delta_2^x u_{j+1/2} = u_{j+1} - 2u_{j+1/2} + u_j, \\ A_0^x u_{j+1/2} &\equiv (E + \Delta_2^x/6) u_{j+1/2} = (u_{j+1} + 4u_{j+1/2} + u_j)/6, \end{aligned} \quad (5)$$

where E is the identity operator. In contrast to [4], operators (5) map functions given on the additional grid ω'_x to functions defined on the joint grid $\omega_x \cup \omega'_x$.

In operator form, Eqs. (2) and (3) become

$$\frac{d}{dt} (A_0^x u_{j+1/2}) + \frac{1}{h_{x,j+1}} \Delta_0^x F_{j+1/2} = 0, \quad j \geq 0, \quad (6)$$

$$\frac{d}{dt} (\Delta_0^x u_{j+1/2}) + \frac{4}{h_{x,j+1}} \Delta_2^x F_{j+1/2} = 0, \quad j \geq 0. \quad (7)$$

Compact difference schemes [6–8] are obtained by discretizing the time derivative in Eqs. (6) and (7) when this evolution system of ordinary differential equations (ODEs) is integrated using either an implicit Euler method or three-stage diagonal implicit Runge–Kutta methods.

3. COMPACT SCHEME FOR A MULTIDIMENSIONAL NONSTATIONARY HYPERBOLIC EQUATION

The method for constructing a compact scheme is described as applied to the two-dimensional analogue of problem (1):

$$\begin{aligned} L_2 u &= 0, \quad L_2 u \equiv \frac{\partial u}{\partial t} + \frac{\partial F(u)}{\partial x} + \frac{\partial G(u)}{\partial y}, \\ a(u) &= \frac{dF(u)}{du} > 0, \quad b(u) = \frac{dG(u)}{du} > 0, \\ u(x, y, 0) &= u^0(x, y), \quad x \geq 0, \quad y \geq 0; \\ u(0, y, t) &= \mu_1(y, t), \quad u(x, 0, t) = \mu_2(x, t), \quad t > 0. \end{aligned} \quad (8)$$

As in the one-dimensional case, a compact scheme for Eq. (8) is constructed using the method of lines combined with an integro-interpolation method. For this purpose, in the domain of spatial variables $\Omega = \{(x, y), x \geq 0, y \geq 0\}$, we introduce a basic grid $\omega_x \times \omega_y$, consisting of integer nodes (x_j, y_k) , where $\omega_y = \{y_k, k \geq 0\}$. Additionally, in this domain, we introduce auxiliary grids $\omega_x \times \omega'_y$, $\omega'_x \times \omega_y$, and $\omega'_x \times \omega'_y$ consisting of half-integer nodes, where $\omega'_y = \{y_{k+1/2}, k \geq 0\}$. Along with baseline equation (8), its differential consequences are also considered:

$$\frac{\partial}{\partial x}(L_2 u) = 0, \quad (9)$$

$$\frac{\partial}{\partial y}(L_2 u) = 0, \quad (10)$$

$$\frac{\partial}{\partial x \partial y}(L_2 u) = 0. \quad (11)$$

By discretizing the spatial derivatives in Eqs. (8)–(11) on the stencil consisting of four integer nodes (x_j, y_k) , (x_{j+1}, y_k) , (x_j, y_{k+1}) , and (x_{j+1}, y_{k+1}) and five auxiliary half-integer nodes $(x_{j+1/2}, y_k)$, $(x_j, y_{k+1/2})$, $(x_{j+1}, y_{k+1/2})$, $(x_{j+1/2}, y_{k+1})$, and $(x_{j+1/2}, y_{k+1/2})$, it is easy to derive four differential-difference equations that hold up to $O(h_{\max}^4)$ for the exact solution of Eq. (8), where $h_{\max} = \max(h_{x,j+1}, h_{y,k+1})$ and $h_{y,k+1} = y_{k+1} - y_k$. The first of these equations has the form

$$\frac{d}{dt} \left(A_0^y A_0^x u_{j+1/2, k+1/2} \right) + \frac{1}{h_{x,j+1}} A_0^y \Delta_0^x F_{j+1/2, k+1/2} + \frac{1}{h_{y,k+1}} A_0^x \Delta_0^y G_{j+1/2, k+1/2} = 0 \quad (12)$$

and approximates the baseline equation (8) on the grid. The other three equations

$$\frac{d}{dt} \left(A_0^y \Delta_0^x u_{j+1/2, k+1/2} \right) + \frac{4}{h_{x,j+1}} A_0^y \Delta_2^x F_{j+1/2, k+1/2} + \frac{1}{h_{y,k+1}} \Delta_0^x \Delta_0^y G_{j+1/2, k+1/2} = 0, \quad (13)$$

$$\frac{d}{dt} \left(A_0^x \Delta_0^y u_{j+1/2, k+1/2} \right) + \frac{1}{h_{x,j+1}} \Delta_0^y \Delta_0^x F_{j+1/2, k+1/2} + \frac{4}{h_{y,k+1}} A_0^x \Delta_2^y G_{j+1/2, k+1/2} = 0, \quad (14)$$

$$\frac{d}{dt} \left(\Delta_0^y \Delta_0^x u_{j+1/2, k+1/2} \right) + \frac{4}{h_{x,j+1}} \Delta_0^y \Delta_2^x F_{j+1/2, k+1/2} + \frac{4}{h_{y,k+1}} \Delta_0^x \Delta_2^y G_{j+1/2, k+1/2} = 0 \quad (15)$$

approximate Eqs. (9)–(11). In Eqs. (12)–(15), the difference operators Δ_0^i , Δ_2^i , and A_0^i ($i = x, y$) are two-dimensional analogues of difference operators (5) and are defined for two-dimensional grid functions

given on the set of half-integer nodes. For example, applying the operators Δ_0^i ($i = x, y$) to the grid functions yields the formulas

$$\begin{aligned}\Delta_0^x u_{j+1/2,k} &= u_{j+1,k} - u_{j,k}, & \Delta_0^x u_{j+1/2,k+1/2} &= u_{j+1,k+1/2} - u_{j,k+1/2}, \\ \Delta_0^y u_{j,k+1/2} &= u_{j,k+1} - u_{j,k}, & \Delta_0^y u_{j+1/2,k+1/2} &= u_{j+1/2,k+1} - u_{j+1/2,k}.\end{aligned}$$

The above manipulations performed for the scalar equation (8) also apply to the system of equations

$$\frac{\partial \mathbf{u}}{\partial t} + \frac{\partial \mathbf{F}(\mathbf{u})}{\partial x} + \frac{\partial \mathbf{G}(\mathbf{u})}{\partial y} = 0,$$

where $\mathbf{u}(x, t)$ is the sought vector function with m components, while $\mathbf{F}(\mathbf{u})$ and $\mathbf{G}(\mathbf{u})$ are given vector functions of dimension m . As a result, we can obtain systems of ODEs similar to (12)–(15).

We introduce a nonuniform grid $\{t_n, n \geq 0\}$ on the interval $[0, \infty)$. Replacing the time derivatives in system (12)–(15) by any difference approximations produces a family of compact difference schemes for the numerical solution of Eq. (8). For example, if the time derivatives at the current level $t = t_{n+1}$ are approximated by backward differences, then we obtain a *baseline* difference scheme consisting of four equations

$$A_0^y A_0^x u_{j+1/2,k+1/2}^{n+1} + r_{x,j+1} A_0^y \Delta_0^x F_{j+1/2,k+1/2}^{n+1} + r_{y,k+1} A_0^x \Delta_0^y G_{j+1/2,k+1/2}^{n+1} = A_0^y A_0^x u_{j+1/2,k+1/2}^n, \quad (16)$$

$$A_0^y \Delta_0^x u_{j+1/2,k+1/2}^{n+1} + 4r_{x,j+1} A_0^y \Delta_2^x F_{j+1/2,k+1/2}^{n+1} + r_{y,k+1} \Delta_0^x \Delta_0^y G_{j+1/2,k+1/2}^{n+1} = A_0^y \Delta_0^x u_{j+1/2,k+1/2}^n, \quad (17)$$

$$A_0^x \Delta_0^y u_{j+1/2,k+1/2}^{n+1} + r_{x,j+1} \Delta_0^y \Delta_0^x F_{j+1/2,k+1/2}^{n+1} + 4r_{y,k+1} A_0^x \Delta_2^y G_{j+1/2,k+1/2}^{n+1} = A_0^x \Delta_0^y u_{j+1/2,k+1/2}^n, \quad (18)$$

$$\Delta_0^y \Delta_0^x u_{j+1/2,k+1/2}^{n+1} + 4r_{x,j+1} \Delta_0^y \Delta_2^x F_{j+1/2,k+1/2}^{n+1} + 4r_{y,k+1} \Delta_0^x \Delta_2^y G_{j+1/2,k+1/2}^{n+1} = \Delta_0^y \Delta_0^x u_{j+1/2,k+1/2}^n. \quad (19)$$

Here, $r_{x,j+1} = \tau/h_{x,j+1}$, $r_{y,k+1} = \tau/h_{y,k+1}$, and $\tau = t_{n+1} - t_n$ is the time step. Difference scheme (16)–(19) is an implicit Euler scheme that is first-order accurate in time and L -stable [13] and, hence, absolutely stable. In what follows, the superscript $n + 1$ on quantities at the current time level is omitted.

Note that the differential-difference equations (12)–(15) were derived by the integro-interpolation method from the conservative differential equations (8)–(11). This equation-deriving technique ensures that the baseline difference scheme (16)–(19) is conservative as well.

Scheme (16)–(19) can be solved using the running calculation algorithm as follows. At the current time level, consider a two-dimensional rectangular corner grid cell with the lower left node at (x_0, y_0) . The values of the grid function u at five nodes (x_0, y_0) , $(x_{1/2}, y_0)$, (x_1, y_0) , $(x_0, y_{1/2})$, and (x_0, y_1) are known from the boundary conditions. Four difference equations (16)–(19) with $j = 0$ and $k = 0$ are used to find the values of u at four nodes $(x_{1/2}, y_{1/2})$, $(x_{1/2}, y_1)$, $(x_1, y_{1/2})$, and (x_1, y_1) . Then similar computations are performed in a neighboring cell in the x or y direction. In fact, scheme (16)–(19) is bicomact in each spatial direction according to the terminology of [14, 15], and the half-integer grid nodes are auxiliary in the scheme. To implement the scheme, the values of the sought function u at half-integer nodes are required only at the initial time level $n = 0$ and on the boundary of the computational domain. Since the scheme is bicomact, its order of accuracy on the integer-valued grid is preserved in the transition from uniform to nonuniform spatial grids.

In the limiting cases when either $F = 0$ or $G = 0$ in Eq. (8), difference scheme (16)–(19) turns into corresponding one-dimensional schemes, which are monotone in a wide range of the local Courant numbers $\kappa_{x,j,k} = a(u_{j,k})r_{x,j}$ and $\kappa_{y,j,k} = b(u_{j,k})r_{y,k}$ (see [6–8]).

A dissipative difference scheme of accuracy $O(\tau^3)$ is obtained when system (12)–(15) is integrated using a special three-stage diagonal implicit Runge–Kutta scheme [8]. Its coefficients \mathbf{A} , \mathbf{b} , and \mathbf{c} [13] are determined by the Butcher tableau

$$\begin{array}{c|ccc} & 1 & & \\ \mathbf{c} & 1/3 & 0 & 1/3 \\ \mathbf{A} & & & \\ \mathbf{b}^T & 1 & -1/12 & 3/4 & 1/3 \\ \hline & & -1/12 & 3/4 & 1/3 \end{array}. \quad (20)$$

This scheme is L -stable and stiffly accurate [13] and involves the baseline scheme of $O(\tau)$ accuracy (the first stage of the scheme).

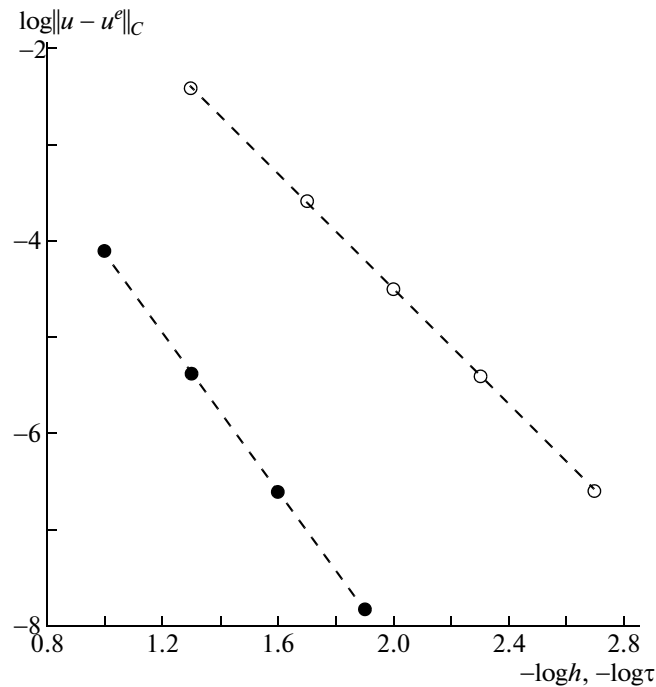


Fig. 1. Error in the numerical solution of the linear advection equation at $t = 1$ as a function of the spatial step h for $\tau = 2 \times 10^{-4}$ (solid circles) and as a function of the time step τ for $h = 5 \times 10^{-3}$ (open circles).

A hybrid monotone scheme is constructed as a nonlinear combination of the baseline scheme of $O(\tau)$ accuracy (scheme A) and scheme (20) of $O(\tau^3)$ accuracy (scheme B). In this scheme, the sought grid function $u_{j,k}$ at the time $t = t_{n+1}$ is computed as a combination of the solution $u_{j,k}(A)$ produced by scheme A and the solution $u_{j,k}(B)$ produced by B (see [7, 8]), specifically,

$$u_{j,k} = \alpha_{j,k} u_{j,k}(A) + (1 - \alpha_{j,k}) u_{j,k}(B), \tag{21}$$

$$0 \leq \alpha_{j,k} = f(C_1 |u_{j,k}(B) - u_{j,k}(A)|/\tau) \leq 1, \tag{22}$$

where $f(w) = w^2/(1 + w^2)$ and $C_1 > 0$ is a constant chosen depending on the problem under study. The choice of the weight functions $\alpha_{j,k}$ in (22) is determined by the behavior of $|u_{j,k}(B) - u_{j,k}(A)|/\tau$ in the domains where the solution is smooth and has jumps. This quantity is $O(\tau)$ and $O(1)$ in the former and latter cases, respectively.

To construct a conservative compact running scheme in the case of the three-dimensional analogue of Eq. (1), namely,

$$L_3 u = 0, \quad L_3 u \equiv \frac{\partial u}{\partial t} + \frac{\partial F(u)}{\partial x} + \frac{\partial G(u)}{\partial y} + \frac{\partial H(u)}{\partial z}, \tag{23}$$

$$a(u) = \frac{dF(u)}{du} > 0, \quad b(u) = \frac{dG(u)}{du} > 0, \quad c(u) = \frac{dH(u)}{du} > 0,$$

along with Eq. (23), we need to consider its differential consequences

$$\frac{\partial}{\partial x}(L_3 u) = 0, \quad \frac{\partial}{\partial y}(L_3 u) = 0, \quad \frac{\partial}{\partial z}(L_3 u) = 0, \tag{24}$$

$$\frac{\partial}{\partial x \partial y}(L_3 u) = 0, \quad \frac{\partial}{\partial x \partial z}(L_3 u) = 0, \quad \frac{\partial}{\partial y \partial z}(L_3 u) = 0, \tag{25}$$

$$\frac{\partial}{\partial x \partial y \partial z}(L_3 u) = 0. \tag{26}$$

Error in the numerical solution of the problem for the linear advection equation with $a = b = 1$, initial conditions (27), and periodic boundary conditions at $r = 0.5$ and $t = 100$

N	E_C	k_C
20	2.51e-2	
40	3.26e-3	2.94
80	4.08e-4	3.00
160	5.10e-5	3.00

By discretizing the spatial derivatives in Eqs. (23)–(26) on a stencil consisting of 8 integer nodes and 19 auxiliary half-integer nodes, it is easy to obtain eight differential-difference equations that hold up to $O(h_{\max}^4)$ for the exact solution of Eq. (23). These equations are similar in structure and difference operators to Eqs. (12)–(15). They can be integrated with respect to time using schemes A and B.

4. GRID CONVERGENCE AND MONOTONICITY OF THE SCHEME

The actual accuracy of the scheme was estimated via computations on refined nested grids (see [11]).

Figure 1 shows the error $u - u^e$ (u^e is the exact solution) computed in the discrete C norm for the numerical solution of problem (8) with $F(u) = G(u) = u$, i.e., for the linear advection equation with $a = b = 1$. The problem was solved in the domain $-1 \leq x, y \leq 1$ with the initial condition

$$u^0(x, y) = \sin(\pi x) \sin(\pi y) \quad (27)$$

and periodic boundary conditions. The grid was uniform with steps $h_x = h_y = h$. The circles in Fig. 1 depict the numerical results and lie on straight lines whose slopes indicate the actual orders of accuracy of three-stage scheme (20). According to Fig. 1, the effective convergence order of the scheme in time is 2.99, while the convergence order in space is 4.11.

Computations were also performed for the linear advection equation over a long time interval on a sequence of refined meshes with the constant value $r = 0.5$ (the ratio of the time step to the spatial mesh

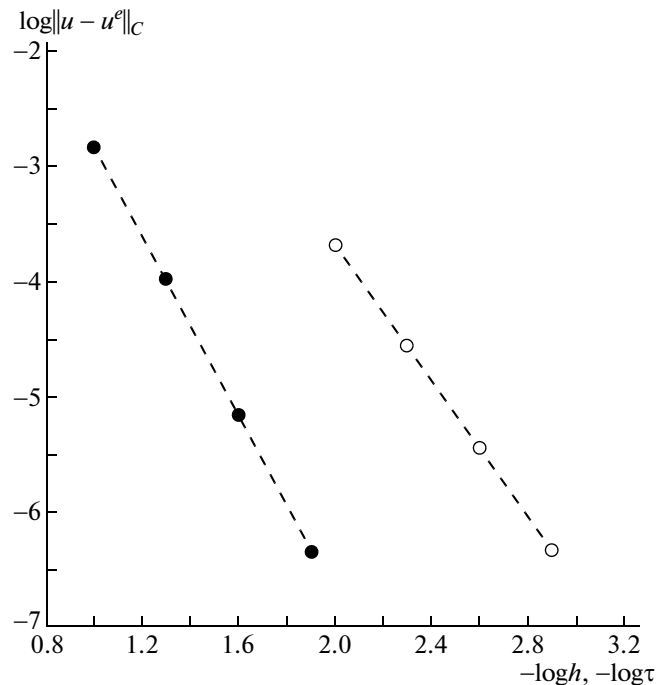


Fig. 2. Error in the numerical solution of the nonlinear Hopf equation at $t = 0.3$ as a function of the spatial step h for $\tau = 2 \times 10^{-4}$ (solid circles) and as a function of the time step τ for $h = 5 \times 10^{-3}$ (open circles).

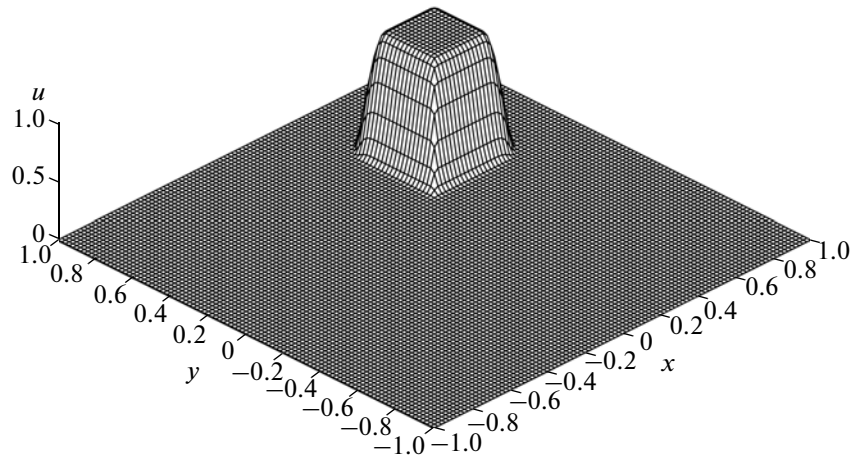


Fig. 3. Numerical results for the propagation of a two-dimensional rectangular pulse at the time $t = 1$ for $h = 10^{-2}$ and the Courant number $\kappa = 0.25$.

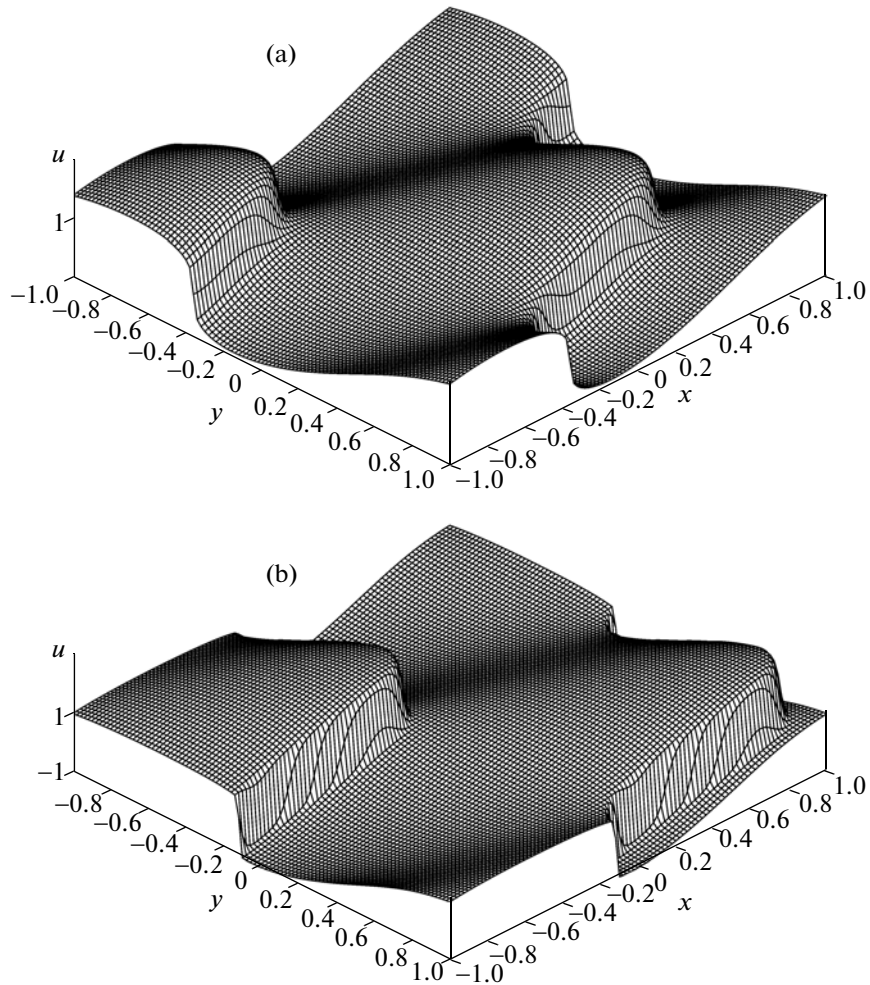


Fig. 4. Numerical solutions of the initial-boundary value problem for the Hopf equation at (a) $t = 2/\pi$ and (b) $t = 0.9$ computed on a uniform grid with $h = 5 \times 10^{-3}$ and the step size ratio $r = 0.5$.

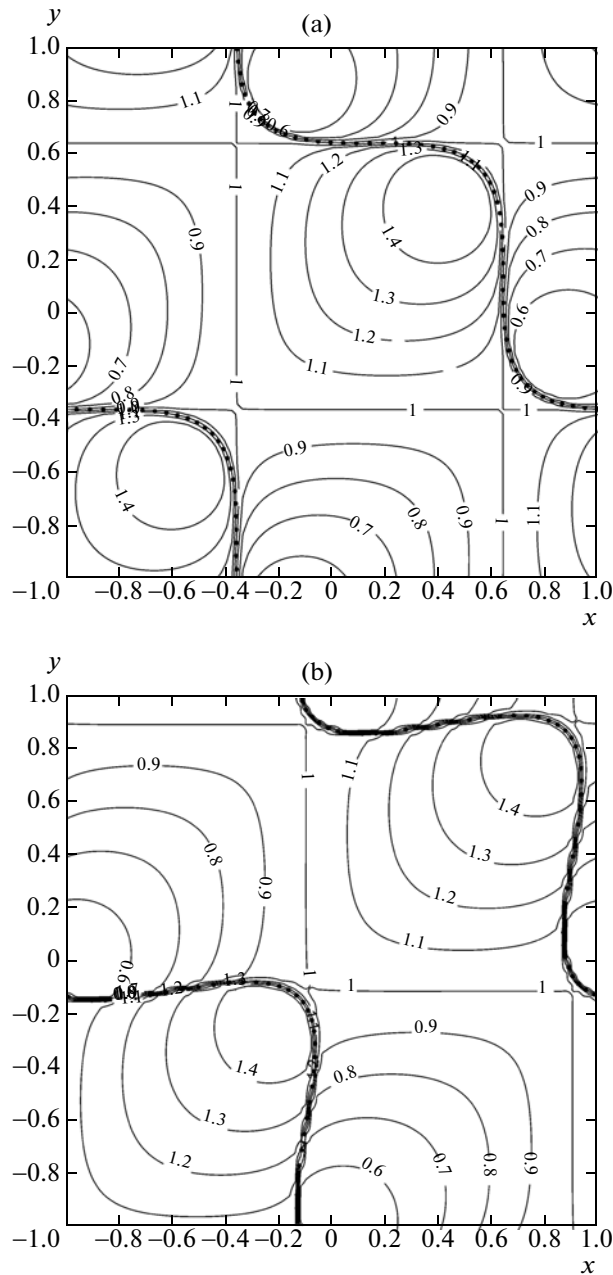


Fig. 5. Contour lines of the numerical solutions to the initial–boundary value problem for the Hopf equation at (a) $t = 2/\pi$ and (b) $t = 0.9$ computed on a uniform grid with $h = 5 \times 10^{-3}$ and the step size ratio $r = 0.5$. The dots show the position of the shock fronts for the exact solution of the problem.

size). The table presents the deviations E_C of the numerical solution from the exact one estimated in the discrete C norm and the convergence orders k_C under mesh refinement:

$$E_C(N, t) = \max_{j,k} |u(x_j, y_k, t) - u^e(x_j, y_k, t)|, \quad k_C(2N, t) = \log_2 \frac{E_C(N, t)}{E_C(2N, t)},$$

where $N = 2/h$ is the number of mesh cells in each spatial direction.

The table shows that the convergence order of the difference scheme on refined meshes in space and time is close to its minimum order of accuracy, i.e., to its order in time.

Figure 2 depicts the error $u - u^e$ in the numerical solution of problem (8) with $F(u) = G(u) = u^2/2$, i.e., for the nonlinear Hopf equation (see [16]). The problem was solved in the domain $-1 \leq x, y \leq 1$ with the initial condition

$$u^0(x, y) = 1 + 0.5 \sin(\pi x) \sin(\pi y) \quad (28)$$

and periodic boundary conditions. The grid was uniform with steps $h_x = h_y = h$. The results presented in Fig. 2 suggest that the effective order of convergence of three-stage scheme (20) in time is 2.94, while the order of convergence in space is 3.88.

Figure 3 displays the numerical results obtained for a two-dimensional rectangular pulse of unit amplitude propagating at the velocities $a = b = 1$. At the initial time $t = 0$, the pulse occupied the domain $-0.7 \leq x, y \leq -0.3$. The problem was solved in the domain $-1 \leq x, y \leq 1$ on a uniform grid with spatial steps $h_x = h_y = h$ by applying hybrid scheme (21), (22) with $C_1 = 2$. Figure 3 shows that the multidimensional scheme yields a nonoscillating solution near the pulse boundary, whose position is well reproduced as a function of time. Thus, the multidimensional scheme inherits the monotonicity of its one-dimensional counterparts (see [6–8]).

For the two-dimensional Hopf equation with initial conditions (28) and periodic boundary conditions, Figs. 4 and 5 depict the numerical solutions produced by hybrid scheme (21), (22) with $C_1 = 1.5$ at the time $t = 2/\pi$, when a jump is formed in the solution [16], and at the time $t = 0.9$, when the jump has a significant height. Figure 4 shows that the compact scheme yields nonoscillating solutions near the jump. The dots in Fig. 5 mark two fronts of discontinuity in the exact solution u^e , at which its spatial derivatives are infinite. In the (x, y) plane, these fronts are parametrically described by the equations

$$\begin{cases} x = \xi + tu^0(\xi, \eta) \\ y = \xi + tu^0(\xi, \eta) \end{cases}, \quad \xi = C_2 - 0.5q, \quad \eta = C_2 + 0.5q,$$

where q is a parameter and C_2 is a constant equal to -1.25 for the first jump in the solution and to -0.25 for the second jump. Figure 5 shows that the positions of the fronts are well reproduced by the difference scheme, which confirms its conservativeness.

Once again, we note that, like the scheme for a scalar one-dimensional equation, the compact scheme proposed for a scalar multidimensional hyperbolic equation can be extended without changes to a system of equations (see [6–8]).

CONCLUSIONS

A compact difference scheme was proposed for the numerical solution of multidimensional nonstationary hyperbolic equations and systems of equations. Due to its construction method, the scheme inherits a number of important properties from its one-dimensional analogue (see [8]).

(i) For smooth solutions, the scheme is fourth-order accurate in space on a stencil consisting of two integer nodes. The half-integer node in the stencil is auxiliary in the sense that it can be eliminated from the scheme on introducing auxiliary grid functions (see [6–8]). In fact, the scheme is bcompact according to the terminology of [14, 15]. As a result, the difference equations of the scheme can be solved by applying the running calculation method. Another consequence is that the order of accuracy of the scheme is preserved on a nonuniform spatial grid consisting of integer nodes.

(ii) The scheme is third-order accurate in time for smooth solutions. It consists of three stages, each represented by a two-level scheme.

(iii) The scheme is absolutely stable.

(iv) The numerical experiments showed that the scheme has monotone numerical solutions in the same wide range of local Courant numbers as its one-dimensional analogues in [6–8]. Moreover, the scheme makes no use of artificial viscosity or monotone procedures in the form of flux limiters.

(v) The scheme is conservative.

(vi) The orders of the scheme in discrete independent variables coincide with those of the differential equations in the respective continuous variables. As a result, the number of boundary conditions for the difference scheme is the same as that for the differential problem to be solved.

(vii) The scheme is efficient. At the current time level, it can be solved by applying the running calculation method in space.

ACKNOWLEDGMENTS

This work was supported by the Russian Foundation for Basic Research (project no. 11-01-00389) and by the Federal Agency for Science and Innovations (state contract nos. 02.740.11.0615 and P594).

REFERENCES

1. A. S. Kholodov, "Numerical Methods for Solving Equations and Systems of Hyperbolic Type," in *Encyclopedia of Low-Temperature Plasmas* (Yanus-K, Moscow, 2008), Vol. VII-1, Part 2, pp. 141–174 [in Russian].
2. A. A. Samarskii and Yu. P. Popov, *Difference Methods for Solving Gas Dynamic Problems* (Nauka, Moscow, 1992) [in Russian].
3. A. S. Kholodov and Ya. A. Kholodov, "Monotonicity Criteria for Difference Schemes Designed for Hyperbolic Equations," *Comput. Math. Math. Phys.* **46**, 1560–1588 (2006).
4. A. I. Tolstykh, *Compact Difference Schemes and Their Application to Aerohydrodynamic Problems* (Nauka, Moscow, 1990) [in Russian].
5. V. V. Ostapenko, "Construction of High-Order Accurate Shock-Capturing Finite-Difference Schemes for Unsteady Shock Waves," *Comput. Math. Math. Phys.* **40**, 1784–1800 (2000).
6. B. V. Rogov and M. N. Mikhailovskaya, "Monotone High-Order Accurate Compact Scheme for Quasilinear Hyperbolic Equations," *Dokl. Math.* **84**, 747–752 (2011).
7. B. V. Rogov and M. N. Mikhailovskaya, "Monotone High-Accuracy Compact Running Scheme for Quasi-Linear Hyperbolic Equations," *Math. Models Computer Simul.* **4**, 375–384 (2012).
8. M. N. Mikhailovskaya and B. V. Rogov, "Monotone Compact Running Schemes for Systems of Hyperbolic Equations," *Comput. Math. Math. Phys.* **52**, 578–600 (2012).
9. V. V. Ostapenko, "Symmetric Compact Schemes with Higher Order Conservative Artificial Viscosities," *Comput. Math. Math. Phys.* **42**, 980–999 (2002).
10. A. I. Tolstykh and D. A. Shirobokov, "Difference Schemes with Fifth-Order Compact Approximations for Three-Dimensional Viscous Gas Flows," *Comput. Math. Math. Phys.* **36**, 477–489 (1996).
11. N. N. Kalitkin, A. B. Al'shin, E. A. Al'shina, and B. V. Rogov, *Computations on Quasi-Uniform Meshes* (Fizmatlit, Moscow, 2005) [in Russian].
12. V. G. Grudnitskii and Yu. A. Prokhorchuk, "A Technique for Constructing Difference Schemes of Any Prescribed Accuracy for Partial Differential Equations," *Dokl. Akad. Nauk SSSR* **234**, 1249–1252 (1977).
13. E. Hairer and G. Wanner, *Solving Ordinary Differential Equations II: Stiff and Differential-Algebraic Problems* (Springer-Verlag, Berlin, 1996; Mir, Moscow, 1999).
14. N. N. Kalitkin and P. V. Koryakin, "Bicompact Schemes and Layered Media," *Dokl. Math.* **77**, 320–323 (2008).
15. B. V. Rogov and M. N. Mikhailovskaya, "Fourth-Order Accurate Bicompact Schemes for Hyperbolic Equations," *Dokl. Math.* **81**, 146–150 (2010).
16. A. D. Polyinin and V. F. Zaitsev, *Handbook of First-Order Partial Differential Equations* (Taylor and Francis, London, 2002; Fizmatlit, Moscow, 2003).

Reproduced with permission of the copyright owner. Further reproduction prohibited without permission.